Remote Sensing of Environment 331 (2025) 115007

Contents lists available at ScienceDirect

Remote Sensing of Environment

journal homepage: www.elsevier.com/locate/rse

Predicting fire-induced individual tree mortality at the landscape level using fire intensity and airborne laser scanning data

Aaron M. Sparks [a,b,*], Ryan Armstrong [b], Alistair M.S. Smith [c], Steve Scharosch [d], Mark V. Corrao [a,b], Thomas Montzka [d]

[a] Department of Forest, Rangeland, and Fire Sciences, College of Natural Resources, University of Idaho, Moscow, ID 83844, USA
[b] Northwest Management Incorporated, Moscow, ID 83843, USA
[c] Department of Earth and Spatial Sciences, College of Science, University of Idaho, Moscow, ID 83844, USA
[d] Delphi Advisors, Boise, ID 83713, USA

ARTICLE INFO

Edited by Zhe Zhu

Keywords:
Fire effects
Fire behavior
LiDAR
Severity
Conifers

ABSTRACT

The prediction of fire-induced tree mortality is important for evaluating potential timber volume losses, replanting costs, and for assessing how mortality will impact long-term yield and carbon dynamics. However, current methods do not provide spatially explicit predictions, limiting the use of this data for proactive forest management, such as thinning and reducing fuel load to reduce tree mortality. In this study we assess whether the incorporation of individual tree inventory data derived from airborne laser scanning and modeled and observed fire intensity data can provide accurate spatially explicit tree mortality predictions. Specifically, tree-level mortality was predicted for over 1.9 million trees within six wildfires in mixed coniferous forest in northwestern Montana, USA, and validated using high resolution imagery for each segmented tree crown. Random forest classification models utilizing observed fire intensity metrics derived from VIIRS observations were the most accurate (overall accuracy: 77.2 %), followed by random forest classification models utilizing modeled fire intensity (64.5–66.1 %) and those that utilized existing logistic regression relationships (55.7–59.0 %). The random forest tree mortality models also produced lower RMSE (6.3–10.2 %) and bias (1.7–3.7 %) compared to the logistic regression approach (RMSE: 38.4 %, bias: −29.6 %) when mortality accuracy was assessed across tree size class. The predictor variable importance quantification showed that fire intensity metrics were more important than species and structural variables in the mortality classification. Ultimately, this study contributes to the remote sensing of fire effects and fire science fields by developing a remote sensing-based methodology for predicting spatially explicit individual tree mortality across large spatial extents.

1. Introduction

Globally, nearly 70 million hectares of forests burn each year, and although there has been a global decline in annual area burned since 2000 (Andela et al., 2017), wildfire activity is projected to increase in many regions in response to climate change (van Lierop et al., 2015; Abatzoglou et al., 2021; Ellis et al., 2022), highlighting the need to improve forecasts of how trees die or recover from fires (Smith et al., 2017). Compounding these projections is the recognition that in many fire-affected ecosystems there is a 'prescribed fire deficit', where more frequent planned fires are needed to maintain ecosystem function (Voelker et al., 2019). Fire effects forecasting is needed by land management personnel to predict immediate and delayed tree mortality, plan salvage operations, evaluate replanting costs, and forecast how surviving fire-affected trees will impact long-term yield, carbon dynamics, and landslide risk (Woolley et al., 2011; Hood et al., 2018). While current tree mortality models can provide accurate mortality predictions in some cases (Cansler et al., 2020; Hood et al., 2018), they rely on on-the-ground observations and are difficult to scale across large areas, hindering their use for proactive forest management (e.g., thinning, fuels reduction, hazard tree removal) (Hood et al., 2018; O'Brien et al., 2018). Given the variable nature of heat flux from fires results in highly variable spatial patterns of fire effects (Sparks et al., 2017; O'Brien et al., 2018), there is a need for a reliable and accurate way to predict tree mortality across spatial scales ranging from the individual tree to the landscape scale.

* Corresponding author at: Department of Forest, Rangeland, and Fire Sciences, College of Natural Resources, University of Idaho, Moscow, ID 83844, USA.
E-mail address: asparks@uidaho.edu (A.M. Sparks).

https://doi.org/10.1016/j.rse.2025.115007
Received 21 July 2025; Received in revised form 29 August 2025; Accepted 2 September 2025
Available online 9 September 2025

Modeling systems that have been parameterized using wildland fire observations provide one avenue to predict tree mortality (Cansler et al., 2020). While current fire-induced tree mortality models provide accurate predictions of immediate mortality in some cases (Cansler et al., 2020; Hood et al., 2018) they are less effective at predicting delayed mortality (Shearman et al., 2023) and do not provide spatial outputs (Hood et al., 2018; O'Brien et al., 2018). Approaches to predict how trees respond to fire have predominately focused on using species-specific pre- and post-fire morphological traits (e.g., bark thickness, crown damage) within logistic-based regressions to predict survival or mortality (Ryan and Reinhardt, 1988; Hood et al., 2018; Rebain, 2022; Woolley et al., 2011). For instance, software widely used by United States fire management personnel include the First Order Fire Effects Model (FOFEM) (Lutes, 2020) and the Forest Vegetation Simulator Fire and Fuels Extension (FVS-FFE) (Rebain, 2022), predict fire-induced tree mortality through logistic regressions. While logistic regression approaches accurately predict species-specific mortality in some cases (>70 % overall accuracy) (Cansler et al., 2020), predictions tend to be biased toward the majority class (Shearman et al., 2019). Other studies have shown ensemble learning algorithms such as random forest (Breiman, 2001) can produce improved results that are unbiased and are more adaptable to new datasets (Shearman et al., 2019). While both of these approaches provide accurate mortality predictions for many species they have not been evaluated whether they can predict mortality accurately across space (O'Brien et al., 2018). Furthermore, current tree mortality models are largely empirically based (Hood et al., 2018), and it is unknown whether they will provide accurate predictions as mortality thresholds shift due to changing climate and compounding stressors, such as drought and extreme heat events (Hood et al., 2018; Kleinman et al., 2019; Dickman et al., 2023).

To overcome these limitations, it has been proposed that models need to include mechanistic information that accounts for heat transfer effects on trees (O'Brien et al., 2018; Dickman et al., 2023). Fire behavior and spread models such as those in the FlamMap fire modeling program (Finney, 2006) could potentially provide fire intensity data for this approach as these models produce spatially explicit fire behavior for specified fuel moisture and weather conditions (Andrews, 1986; Finney, 2006). FlamMap derived simulations may not produce as accurate spread rates and heat flux compared with physics-based computational fluid dynamics models that are linked to the atmosphere (e.g., WFDS, Mell et al., 2007; QUIC-fire, Linn et al., 2020). However, FlamMap simulations do not require high resolution 3-D fuel datasets and high performance computing resources needed by these models at large spatial scales and as such are more relevant to managers with limited fuels data and computational resources. Some studies have used modeled fire intensity derived from FlamMap to predict tree mortality (Ager et al., 2007, 2010; Alcasena et al., 2016). However, in most cases tree mortality was predicted at the stand level which masked any intra-stand mortality patterns, and importantly, no validation was completed in any of these studies to quantify the accuracy of the tree mortality predictions. Recent pyroecophysiology studies (Smith et al., 2025) that subject trees to known levels (i.e., doses) of heat flux via surface fires have shown that post-fire plant physiology, growth, and mortality of many tree species and tree sizes vary as a function of remotely sensed fire intensity measures like fire radiative power (FRP, units: W m^{-2}) and its temporal integral, fire radiative energy (FRE, units: J m^{-2}) (Smith et al., 2017; Steady et al., 2019; Sparks et al., 2018, 2023a, 2023b). Incorporating remotely sensed fire intensity data into mortality prediction holds significant promise for improving mortality estimates (Hood et al., 2018; O'Brien et al., 2018) but its ability to predict spatial patterns of fire-induced mortality has not been assessed.

Incorporating fire intensity data with airborne laser scanning data could potentially enhance the ability of current and new approaches to produce spatially explicit individual tree mortality predictions (Sparks et al., 2023b). Individual tree inventories derived from airborne laser scanning (ALS) data have been shown to detect most overstory trees (dominant and codominant trees) (Falkowski et al., 2008; Vauhkonen et al., 2012; Sparks et al., 2022, 2024a). This spatially explicit individual tree information could be combined with either modeled or observed fire intensity data to predict individual tree mortality. Fire intensity metrics such as fire radiative power are currently acquired on a range of spatial scales using airborne (e.g., Hudak et al., 2015; Schroeder et al., 2014a) and satellite platforms (Giglio et al., 2016; Schroeder et al., 2014b). For example, the Visible Infrared Imaging Radiometer Suite (VIIRS) sensor aboard the NASA/NOAA Suomi National Polar-orbiting Partnership (Suomi-NPP) and NOAA-20/21 satellites can provide up to six active fire observations at mid-latitudes at 375 m spatial resolution (Schroeder et al., 2014b). Recent studies have used multitemporal ALS-derived tree height data and remotely sensed fire radiative power data to quantify fire intensity impacts on post-fire mature tree growth (Sparks et al., 2023b). Other studies have assessed the relationship of fire radiative power derived from the VIIRS predecessor, the Moderate Resolution Imaging Spectroradiometer (MODIS) sensor onboard the Terra and Aqua satellites, and forest net primary productivity (Sparks et al., 2018). However, to the authors' knowledge no studies have coupled ALS-derived individual tree inventories and fire intensity datasets for mortality prediction.

The need for tree-level mortality prediction methods has grown in recent decades to meet the information requirements of various management activities including: planning silvicultural treatments and salvage operations in mixed conifer forests that include species of varying fire susceptibilities (Cansler et al., 2020), planning fuel reduction around old, relic trees that are susceptible to fire-induced mortality (Hood, 2010; Flanary and Keane, 2020; Shive et al., 2022), and removing potential hazard trees around recreation areas and powerlines (Ahmed et al., 2013; Cansler et al., 2020). For applications that need predictions well in advance of planned and unplanned fires, approaches that use modeled fire intensity would clearly be more useful than approaches that use observed fire intensity. However, approaches that use observed fire intensity could provide useful information on where actions could be taken to reduce delayed mortality, which can occur many years after the fire (Youngblood et al., 2009), as well as inform post-fire remediation planning. To address these research needs, the overall objective of this study was to evaluate the ability of three spatially explicit approaches to predict post-fire individual tree mortality in an ALS-derived individual tree inventory of over 1.9 million trees. The three approaches included a logistic regression approach that used FlamMap modeled fire intensity and crown scorch-mortality probability relationships to predict individual tree mortality (hereafter the 'LR-FM' approach), a random forest classification approach that used FlamMap modeled fire intensity and individual tree ALS-derived structural metrics to predict individual tree mortality (hereafter the 'RF-FM' approach), and a random forest classification approach that used VIIRS-derived fire intensity metrics and individual tree ALS-derived structural metrics to predict individual tree mortality (hereafter the 'RF-VIIRS' approach). Specifically, this study sought to 1) quantify the accuracy of the three approaches to predict fire-induced mortality, 2) characterize how prediction accuracy changes with tree size and time since fire, 3) identify and discuss the utility and limitations of each approach for research and natural resource management applications.

2. Study area and data

2.1. Study area

This study was conducted in the Flathead Reservation in northwestern Montana, USA (Fig. 1). The study area encompasses a range of forest types ranging from dry, low elevation mixed conifer forest to wet, high elevation mixed conifer forest in the Mission Mountains (LANDFIRE: LANDFIRE Existing Vegetation Type layer, 2023). This study focuses on six fires that burned in 2022–2023 in which collocated pre-fire ALS data, post-fire high resolution imagery, and VIIRS active fire

Fig. 1. Location of the six study fires within the Flathead Reservation in northwestern Montana, USA. A Landsat 8 false color composite (red: B7, green: B5, blue: B2), acquired August 29, 2023, is used as background to highlight the distribution of forest (dark green), agriculture (light green), shrubland and senesced herbaceous vegetation (brown), and burned areas (dark red). (For interpretation of the references to color in this figure legend, the reader is referred to the web version of this article.)

observations are available. The fires ranged from 14 to 8384 ha in size. Two of the fires occurred in 2022 (Garceau, Red Horn) and four occurred in 2023 (Niarada, Middle Ridge, Communication Butte, Holmes). Four of the fires burned in low elevation (~1100–1650 m), mixed conifer forests dominated by *Pseudotsuga menziesii* and *Pinus ponderosa* (Niarada, Garceau, Middle Ridge, Communication Butte) (Fig. 1, left side). Two of the fires burned in high elevation (~2160–2260 m) mixed conifer forest dominated by *Picea englemanii* and *Abies lasiocarpa* in the Mission Mountains (Holmes, Red Horn) (Fig. 1, right side).

2.2. ALS derived individual tree inventory

Pre-fire ALS data was acquired across the entire study area in September 2021 using a RIEGL VQ-1560II sensor (RIEGL Laser Measurement Systems, Horn, Austria) with a 58-degree field-of-view. The sensor was mounted on a fixed-wing aircraft that varied its elevation between 1600 and 1900 m above ground level to produce 55 % flightline overlap. The ALS data had an average pulse density of twenty pulses per square meter (ppm) and an average of four per-pulse returns over forested areas. Laser intensity normalization and return classification was completed by the supplier prior to delivery of the data following the American Society for Photogrammetry and Remote Sensing classification standard (ASPRS, 2011).

The ALS data was used to derive an individual tree inventory spanning the six study fires. ForestView, a "gray box" tree detection and measurement software developed by Northwest Management Incorporated (NMI, Moscow, Idaho), was used to detect individual trees (Corrao et al., 2022; Sparks and Smith, 2022a). ForestView uses local maximum filtering and watershed segmentation to detect peaks in ALS point cloud-derived canopy height models (CHM). Detected peaks that are at least 2 m in height are assumed to be treetops. In addition to detection of trees, the software uses an internal database of field- and ALS-measured trees, along with point cloud derived metrics (e.g., height percentiles, stratified return densities, crown shape, laser return intensity) to model diameter at breast height (DBH) and predict species and live or dead status for each detected tree (Corrao et al., 2022). ForestView tree detection accuracies have been found to be comparable to other methods, with a higher proportion of dominant and codominant trees detected (>70 % on average) than intermediate and suppressed trees (<31 % on average) (Sparks and Smith, 2022; Corrao et al., 2022; Sparks et al., 2022). Likewise, an independent assessment reported that ForestView species classification for dominant species in a similar mixed conifer forest had relatively high classification accuracies (Producer's accuracy: 60–68 %, User's accuracy: 56–78 %) (Sparks and Smith, 2022).

In total, 2,979,276 trees were detected within the six study fires, and each tree was given a unique identification code. Given that competition is a significant driver of reduced growth and increased mortality (Contreras et al., 2011; van Mantgem et al., 2016), the Hegyi (1974) distance-dependent competition index was also calculated for each tree in the individual tree inventory as follows:

$$Hegyi\ competition\ index = \sum_{i=1}^{n} \frac{DBH_i}{DBH \times d_i} \quad (1)$$

where DBH is the DBH of the target tree, DBH_i is the DBH of the *i*th neighbor tree, and d_i is the horizontal distance between the target tree and the *i*th neighbor tree. Following Lorimer (1983), the search radius around each tree was 14 m, which is 3.5 times the average crown radius in the individual tree inventory.

2.3. High resolution imagery

Post-fire sixty-centimeter spatial resolution airborne imagery from the National Agriculture Imagery Program (NAIP) was used to classify the proportion of dead canopy within each ALS-segmented crown. These data consisted of 4-band imagery (blue, green, red, near-infrared) acquired in early September of 2023. NAIP imagery is collected under contract specifications that allow up to 10 % cloud cover and is balanced for contrast and color and orthorectified using digital elevation models (Maxwell et al., 2017). No clouds, smoke or haze were visible in the imagery used in this study.

2.4. VNP14IMG active fire product and preprocessing

The VNP14IMG active fire product was used to map the fire intensity, in terms of fire radiative power and fire radiative energy, across each of the six study fires. The VNP14IMG active fire product is derived from the Visible Infrared Imaging Radiometer Suite (VIIRS) sensor aboard the NASA/NOAA Suomi National Polar-orbiting Partnership (Suomi-NPP) and NOAA-20/21 satellites (Schroeder et al., 2014b). VIIRS observes Earth's surface twice each day with equatorial overpasses at 1:30 am and 1:30 pm. VIIRS data undergoes a pixel aggregation process, whereby pixels are aggregated at lower scan angles to limit the pixel area increase with scan angle (Wolfe et al., 2013). The VIIRS active fire product uses the VIIRS 375 m 'I-bands' and 750 m 'M-bands' and has a spatial resolution of 375 m at nadir, which results in an active fire sensitivity of around 10 times that of the Moderate Resolution Imaging Spectroradiometer (MODIS) (Zhang et al., 2017; Wooster et al., 2021). The 375 m I-bands are used primarily for fire detection and the 750 m M-bands are used in sub-pixel FRP retrieval (Schroeder and Giglio, 2016) due to frequent fire pixel saturation in the I-bands (Schroeder et al., 2014b). FRP retrieval for each 750 m fire pixel is estimated following Wooster

et al. (2003) and is divided among the number of coincident 375 m fire pixels. The final 375 m spatial resolution product includes a fire mask, quality assurance data and FRP.

Several preprocessing steps were used to map FRP and FRE across each of the study fire extents. We used maximum FRP and FRE as both metrics have been linked with reduced post-fire mature tree growth and productivity (Sparks et al., 2018; Sparks et al., 2023b). Following Sofan et al. (2020), we buffered each active fire pixel centroid by the average of the along-track and along-scan pixel size divided by two (i.e., observations at nadir would have buffer of 187.5 m), resulting in overlapping observations. Maximum FRP was identified for each area with overlapping observations. FRE was calculated as the temporal integral of FRP, assuming that FRP varies linearly between observations (Boschetti and Roy, 2009). VIIRS observation summary statistics for all fires are shown in Fig. 2.

2.5. Fire modeling input data

FlamMap 6.2 (Finney, 2006) was used to model fire behavior across the entire study area. FlamMap requires topographic data (elevation, slope, aspect), fire behavior fuel models, forest canopy characteristics (cover, height, crown base height, crown bulk density), fuel moisture and weather data. All input datasets were generated at- or resampled to-90 m spatial resolution.

Elevation, aspect, and slope data for the study area were derived from 10 m spatial resolution digital elevation models in the National Elevation Dataset (Gesch et al., 2002). These data were resampled using bi-linear resampling to 90 m resolution to match the other input datasets. The Forest Vegetation Simulator Fire and Fuels Extension (FVS-FFE) (Rebain, 2022) was used to assign a standard fire behavior fuel model (Scott and Burgan, 2005) to each grid cell. FVS-FFE assigns two or more fire behavior fuel models to a cell, based on stand characteristics and fuel loads. Fire behavior parameters are predicted separately for each selected fuel model, and then combined into weighted averages using the relative difference in stand fuel loadings and the selected reference fuel models. FVS-FFE selects multiple fuel models for predicting fire behavior to reduce the potential for dramatic changes in predicted fire behavior from one simulation growth cycle to the next, when relatively small changes in stand attributes cause the stand to move from one fuel model to another.

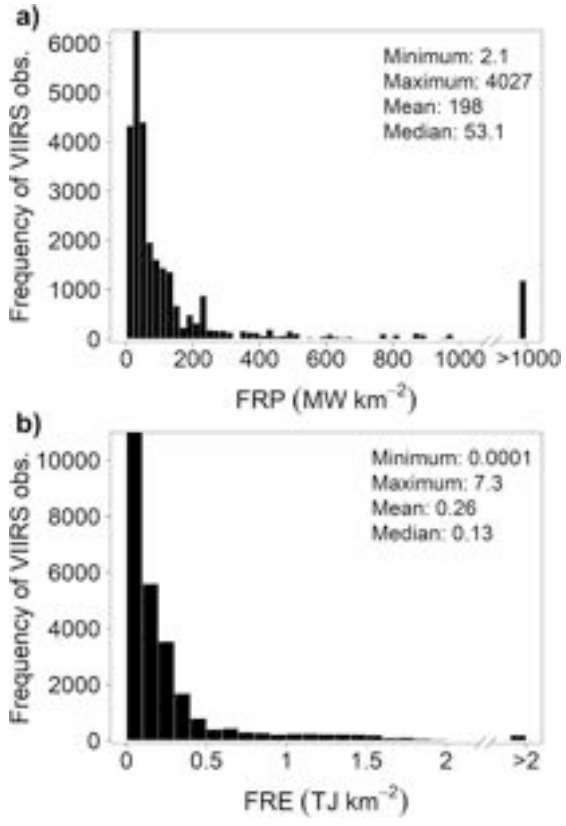

Fig. 2. Distributional statistics of (a) fire radiative power (FRP) and (b) fire radiative energy (FRE) across all study fires.

Forest canopy inputs were modeled using the ALS-derived individual tree inventory and FVS-FFE. Canopy height was calculated by FVS as the mean height of the dominant trees within a grid cell. FVS-FFE was used to compute percent canopy cover by summing the projected crown areas of the individual trees. Crown bulk density for each tree was calculated in FVS-FFE using Brown's (1978) equations for Rocky Mountain conifers and then averaged to the 90 m grid cell. Crown base height (CBH) was calculated individually for each tree and was defined as the lowest height where canopy bulk density was at least 0.005 kg m^{-3}. For the FlamMap simulations, CBH was averaged to the 90 m grid cell.

Fuel moisture and wind speeds were calculated using the average daily fuel moisture and wind speed values from the four RAWS weather stations within the study area. The 80th and 95th percentiles of observed values were computed using the FireFamily Plus software package (FireFamily+, 2024) and are presented in Table 1. Computations were based on hourly weather data from 2004 to 2024, filtered for the date range May to September, of each year. Data from all four RAWS stations were combined into pooled data estimates, using equal weightings for all four stations. The 80th and 95th percentile weather conditions were used as they span conditions associated with less intense fire behavior to more intense fire behavior that is associated with detrimental impacts to ecological, economic, and social values (Bowman et al., 2017).

3. Methods

3.1. Overview

Three main steps were needed to address the study objectives and are outlined in Fig. 3. In the first step, we generated a reference live or dead dataset using the ALS-derived individual tree inventory and high resolution NAIP imagery that could be used for training and validation of each of the three mortality modeling approaches. This step was only conducted on trees identified as live in the pre-fire ALS-derived individual tree inventory so that we could reduce the probability that observed tree mortality was due to other factors besides the wildfires. In the second step, we modeled fire behavior at 90 m spatial resolution across the study area using FlamMap and structural information from the pre-fire ALS-derived individual tree inventory and historical weather conditions for the study area (e.g., 80th and 95th percentile fuel moisture and windspeed). In the final step, we predicted and validated mortality for each tree in the reference dataset using three modeling approaches. Each modeling approach used predictor variables that are known to be associated with fire-induced tree mortality (e.g., fire

Table 1
Weather and fuel moisture content values used in the study area-wide fire simulations representing 80th and 95th percentile conditions. Most common wind direction is also reported.

Variable	80th percentile conditions	95th percentile conditions
Windspeed (km h^{-1})	11.3	14.5
Wind direction (°)	203	275
1-h fuel moisture (%)	5	4
10-h fuel moisture (%)	6	4
100-h fuel moisture (%)	9	7
Live herb. Moisture (%)	33	30
Live woody veg. Moisture (%)	73	60

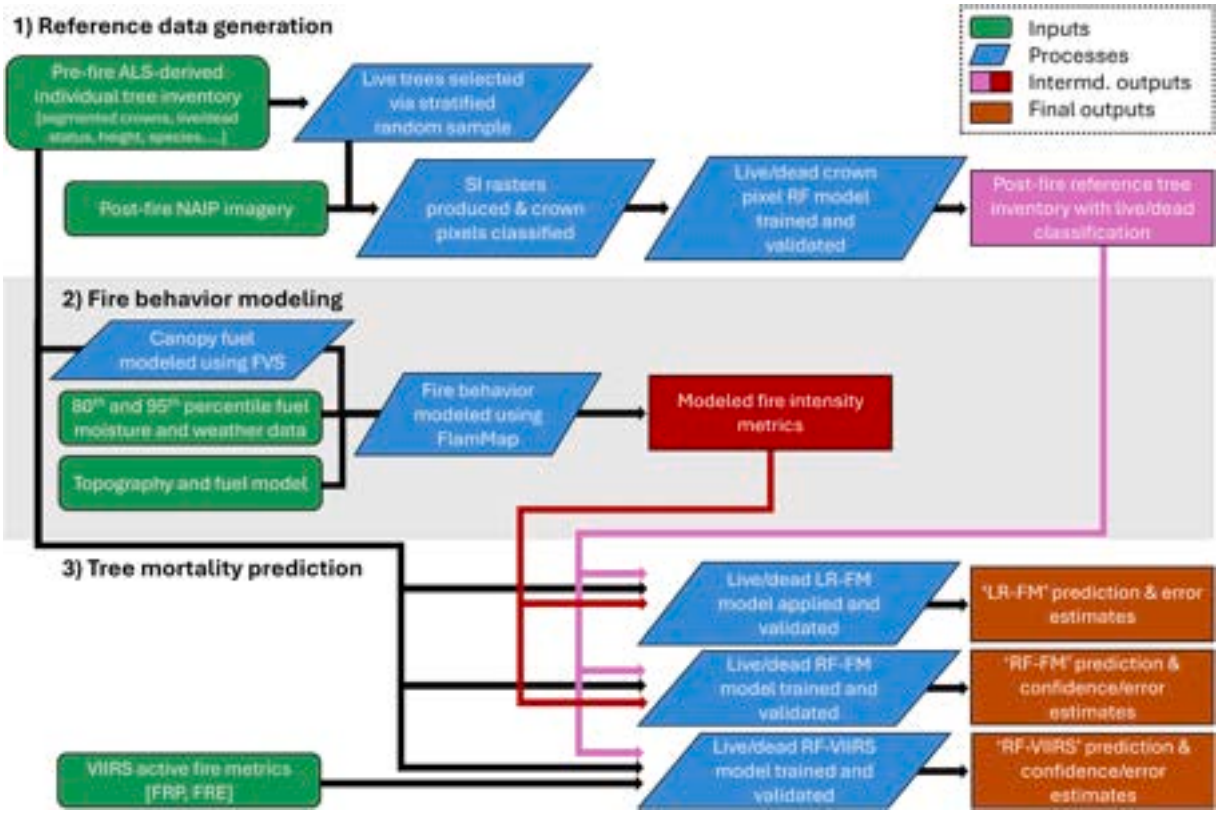

Fig. 3. Study framework highlighting the main inputs, processes, intermediate outputs and final outputs associated with the three main methodological steps.

intensity, tree size, crown base height and species). The 'LR-FM' and 'RF-FM' approaches used FlamMap-modeled fire intensity metrics and the 'RF-VIIRS' approach used observed fire intensity derived from VIIRS active fire observations. Accuracy of each modeling approach was quantified by comparing the predicted individual tree mortality with observed mortality from the reference dataset at the individual tree scale and across tree size class and space. A distance-to-second-class metric using the predicted class probabilities from the RF models was also computed and compared with observed error to explore if this metric could provide useful information on classification confidence. A detailed description of each step is provided in the following sections.

3.2. Reference data generation: Individual tree crown classification

A random forest classification approach was used to classify pixels within each ALS-segmented tree crown as 'live', 'unconsumed dead', 'consumed dead', and 'shadow' classes. The 'unconsumed dead' class included pixels with scorched foliage that appear yellow or brown and the 'consumed dead' included pixels where foliage was consumed, and only the main stem and charred branches remained. Random forest is an ensemble learning algorithm that aggregates the results of an ensemble of n classification trees trained using bootstrapped samples of the training data (Breiman, 2001). Crown pixels are assigned a classification by a majority vote of the ensemble of classification trees and cross-validated using "out-of-bag observations", which are data not included in the bootstrap samples. Predictor variables included individual NAIP bands (blue, green, red, near-infrared) and spectral indices known to be sensitive to photosynthetically active vegetation (Table 2).

Reference data used for training and validation was selected using a stratified random sampling approach. Mean tree height and density were calculated using the individual tree inventory for each 90 m grid cell of the fire behavior modeling grid. We selected 90 m grid cells across the tree height and density range to capture variability in stand structure and illumination conditions (older, structurally complex forest stands will likely have more shadow within and among tree crowns than younger forest stands). Grid cells were grouped into strata by three height and density percentile classes (0–33, 33–66, 66–100), resulting in nine total strata. Five 90 m grid cells were randomly selected within each of the nine strata, and all 60 cm tree crown pixels within a selected grid cell were manually classified using visual interpretation of natural color (red: Red band, green: Green band, blue: Blue band) and false color (red: NIR band, green: Red band, blue: Green band) high-resolution imagery composites and guided by the pre-fire ALS-segmented crown polygons. The tree crown reference dataset consisted of 24,391 'live' samples (pixels), 32,186 'unconsumed dead' samples, 35,617 'consumed dead' samples, and 1725 'shadow' samples

The 'randomForest' (Liaw and Wiener, 2002) R package in R statistical software (R Core Team, 2024) was used for tree crown classification. The classifier was parameterized using a number of decision trees (Ntree) of $n = 500$ trees, and the number of predictor variables selected at each split (Mtry) was set to the number of predictor variables divided by three. Other studies have observed large variability in classification accuracy when a single split is used to separate the reference data into

Table 2
Spectral index formulation and associated reference.

Spectral Index	Formula	Reference
Red-Green Index	$RGI = \frac{\rho_{red}}{\rho_{green}}$	Coops et al., 2006
Ratio Vegetation Index	$RVI = \frac{\rho_{NIR}}{\rho_{red}}$	Pearson and Miller, 1972
Normalized Difference Vegetation Index	$NDVI = \frac{\rho_{NIR} - \rho_{red}}{\rho_{NIR} + \rho_{red}}$	Rouse et al., 1974

ρ_λ denotes reflectance in spectral band λ: ρ_{green} = green reflectance, ρ_{red} = red reflectance, ρ_{NIR} = near infrared reflectance.

training and validation datasets (Lyons et al., 2018). In an effort to minimize this variability, bootstrapping was used to repeatedly draw a random 10 % sub-sample from the reference dataset and split these sub-sample reference datasets into training and validation sets using an 80:20 ratio. In total, 100 different sets were generated and classified. Confusion matrices generated between the predicted classification and the reference observations were used to calculate overall accuracy and omission and commission errors.

The majority classification value from the 100 different classification sets was used as the final crown classification and was used to generate a reference dataset of live and dead trees. Following Stovall et al. (2019) and Hemming-Schroeder et al. (2023) individual trees were considered dead if at least 37 % of the tree crown was classified as dead, as these studies found this threshold was the most accurate and unbiased for mortality classification in western U.S. conifers. This 'live' or 'dead' dataset served as the reference dataset for training and validating the tree mortality modeling approaches and consisted of 885,670 live trees and 2,093,606 dead trees.

3.3. Fire behavior modeling

We used FlamMap 6.2 (Finney, 2006) to model fire behavior for all 90 m grid cells within our study area. FlamMap uses input surface and tree canopy fuel data, topography, weather data and fire behavior models (Rothermel, 1972; Andrews, 1986) to produce grid cell predictions of fire spread rate, flame length, crown fire activity type, fireline intensity and heat release per unit area. Fire behavior was modeled for all grid cells using the input data (detailed in section 2.4.) and fireline intensity (kW m^{-1} s^{-1}) and heat per unit area (kW m^{-2}) outputs were used in the tree mortality modeling (detailed in 3.4.1. and 3.4.2.).

3.4. Individual tree mortality modeling

Tree mortality was modeled using three approaches, detailed in the following sections. For comparison purposes, only trees that were collocated with both FlamMap modeled fire behavior and VIIRS observations were modeled and compared. Of the total 2,979,276 trees in the reference dataset, 1,921,218 trees greater than 2 m in height were collocated and considered in the following analyses with 632,741 trees being labeled as 'live' and 1,288,477 trees being labeled as 'dead'. The height distribution of these trees is shown in Fig. 4.

3.4.1. Logistic regression approach

The logistic regression approach to modeling individual tree mortality used methodology similar to that in FVS-FFE. Two model runs were performed: the first used fireline intensity generated using 80th percentile fuel moisture and weather conditions, and the second used fireline intensity generated using 95th percentile fuel moisture and weather conditions. The FlamMap modeled fireline intensity was used to estimate crown scorch height. This information was coupled with species and bark thickness data in published species-specific logistic regression models (Cansler et al., 2020) to predict the probability of mortality for each tree. Crown scorch height (H_s: m) was calculated following van Wagner (1973):

$$H_s = 0.1483 \times I^{0.667} \quad (2)$$

where I is the fireline intensity in kW m^{-1}. The total crown scorch proportion was calculated following Peterson and Ryan (1986). Bark thickness of each tree in the individual tree inventory was calculated by multiplying species specific bark thickness coefficients in Cansler et al. (2020) by the DBH. Crown scorch proportion and bark thickness were used as inputs in published species-specific logistic regression models compiled by Cansler et al. (2020) to estimate the probability of mortality. Recommended mortality probability thresholds from Cansler et al. (2020) were used to predict whether a tree was living or dead. Validation was conducted using confusion matrices calculated between the predicted live or dead classification and the reference live or dead dataset.

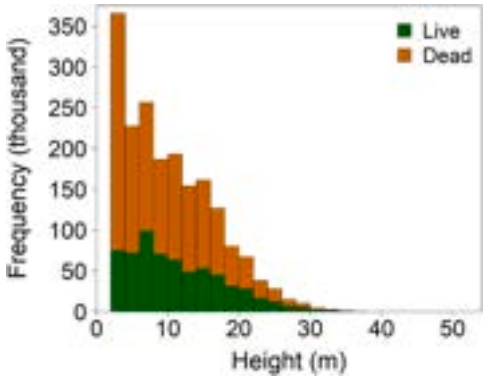

Fig. 4. Height distribution of live and dead trees selected from the reference dataset for tree mortality modeling.

3.4.2. Random forest approaches

Two random forest classification models were used to predict each tree's live or dead status using ALS-derived structural data and fire intensity metrics. Both random forest models used species and structural predictor variables known to be associated with fire-induced tree mortality. These included tree height, CBH modeled using FVS-FFE, Hegyi competition index value and species. The first model (RF-VIIRS) used VIIRS-derived maximum FRP and FRE in addition to structural predictor metrics. The second model (RF-FM) used FlamMap-derived heat per unit area in addition to structural predictor metrics. Two model runs were performed: the first used heat per unit area generated using 80th percentile fuel moisture and weather conditions, and the second used heat per unit area generated using 95th percentile fuel moisture and weather conditions.

Random forest classification was conducted using the 'randomForest' (Liaw and Wiener, 2002) R package in R statistical software (R Core Team, 2024). Bootstrapping was used to repeatedly draw a random 10 % sub-sample from the reference dataset and split these sub-sample reference datasets into training and validation sets using an 80:20 ratio. In total, 100 different sets were generated and classified. Predictor importance was computed for each classification iteration as the normalized difference in the misclassification rate between the original classification and a modified classification where values of the predictor variable were randomly permuted in the out-of-bag observations. Validation was conducted for each classification iteration using confusion matrices calculated between the predicted live or dead classification and the reference live or dead dataset.

3.4.3. Uncertainty quantification and class attribution confidence analysis

In addition to the classification accuracy computed using confusion matrices (Sections 3.4.1. and 3.4.2.) we assessed the accuracy of mortality estimates binned into 2 m height classes using the average root mean square error (RMSE) (Eq. 3) and mean bias (Eq. 4):

$$RMSE = \sqrt{\frac{\sum_{i=1}^{n}(\hat{x} - x_i)^2}{n}} \quad (3)$$

$$Mean\ bias = \frac{\sum_{i=1}^{n}(\hat{x} - x_i)}{n} \quad (4)$$

where $\hat{x}$ are the predicted mortality values, x_i are the observed mortality values, and n is the number of observations. We computed these accuracy measures considering all trees and considering 2022 and 2023 fires

separately to assess if there were any differences in immediate and delayed mortality quantification. We also calculated the proportion of total mortality (all size classes) for each 90 m grid cell within each fire perimeter to provide an aggregated accuracy measure that could be used to qualitatively assess spatial mortality pattern agreement. Aggregated mortality error was calculated as predicted mortality minus observed mortality for each grid cell. Summary statistics calculated using the distribution of errors between observed and predicted mortality were used to assess agreement.

We also conducted a distance-to-second-class (D2SC) analysis following Mitchell et al. (2008) and Hermosilla et al. (2022) using the predicted class probabilities from the RF models to see if this metric could provide useful information on classification confidence. D2SC is computed as follows (Eq. 5):

$$D2SC = 100 \times \left(1 - \frac{c_2}{c_1}\right) \quad (5)$$

where c_1 is the proportion of votes of the most voted class and c_2 is the proportion of votes of the second most voted class. Values of D2SC closer to 0 indicate lower class attribution confidence while values closer to 100 indicate higher class attribution confidence. Grid cell error was compared with mean D2SC for each grid cell to quantify the trend and variability in classification error with increasing classification confidence.

4. Results

4.1. Reference data generation: Individual tree crown classification

The overall accuracy of the crown classification, averaged over the 100 dataset iterations, was 81.4 % (±0.1 %) (Table 3). Average omission errors were lowest for the live class (6.4 %) and higher for dead (21.0–24.3 %) and shadow (30.5 %) classes. Likewise, average commission errors were lowest for the live class (9.4 %) and higher for dead (21.4–24.9 %) and shadow (19.3 %) classes (Table 3). An example of the crown classification and tree status attribution is shown in Fig. 5. Specifically, Fig. 5 shows a post-fire false color NAIP composite (red: NIR band, green: red band, blue: green band) (Fig. 5a), crown classification (Fig. 5b), and tree status attribution (Fig. 5c) for an area within the 2023 Niarada fire with a mixture of healthy trees, scorched trees, and trees with consumed foliage. The classified crown results showed close correspondence to visual patterns of crown death and consumption observed in the post-fire NAIP imagery for most of the fires. However, older fires (Garceau, Red Horn) had small areas where understory regeneration underneath consumed tree crowns resulted in these dead trees being misclassified as 'live'. The assessment of predictor variable importance shows that the Red-Green Index and the blue band were more important for the crown classification than the other bands (red, green, NIR) and spectral indices (NDVI, RVI) (Fig. 6).

Table 3
Confusion matrix results showing crown classification accuracy, averaged across the 100 classification iterations. Accuracy metrics report the mean (±95 % confidence interval).

Classification	Accuracy metric	Mean value (%) (±95 % CI)
Live	Omission error	6.4 (0.1)
	Commission error	9.4 (0.2)
Dead (unconsumed)	Omission error	21.0 (0.3)
	Commission error	24.9 (0.2)
Dead (consumed)	Omission error	24.3 (0.3)
	Commission error	21.4 (0.3)
Shadow	Omission error	30.5 (0.4)
	Commission error	19.3 (0.4)
	Overall accuracy	81.4 (0.1)

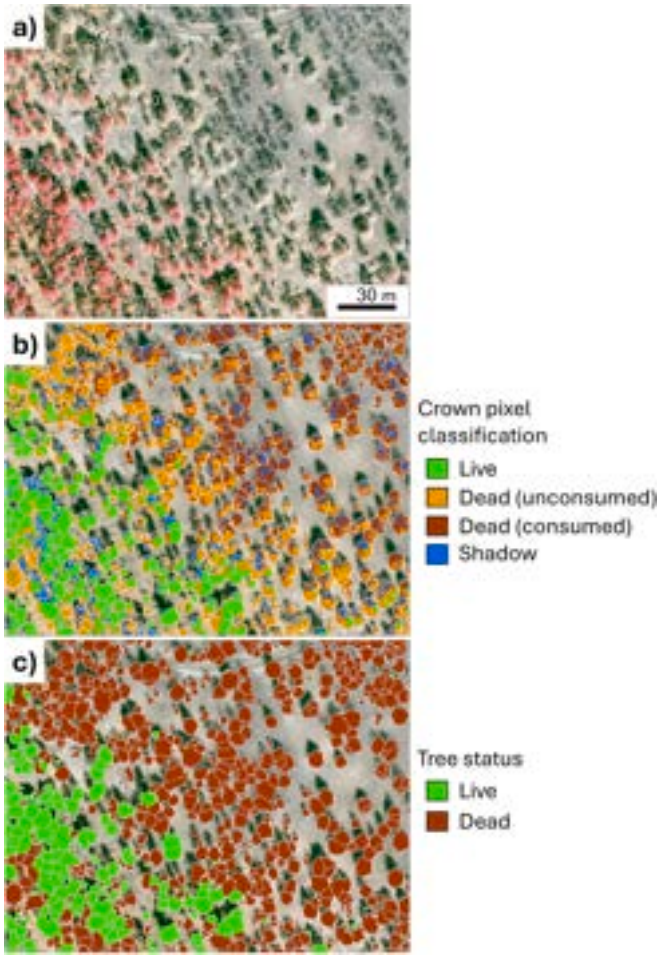

Fig. 5. Crown classification and tree status attribution for an area within the 2023 Niarada fire with a mixture of healthy trees, scorched trees, and trees with consumed foliage. Panel (a) shows a post-fire false color NAIP composite (red: NIR band, green: red band, blue: green band) acquired in September 2023. Non-scorched foliage appears red. Scorched foliage appears yellow to brown and consumed foliage appears gray to black. Panel (b) shows the results of the crown classification and panel (c) shows the tree status, where trees with >37 % of dead crown are considered dead. ALS-segmented tree crowns are displayed in white on all panes. (For interpretation of the references to color in this figure legend, the reader is referred to the web version of this article.)

4.2. Mortality prediction

The overall accuracy of the individual tree mortality predictions was 55.7–59.0 %, 64.5–66.1 %, and 77.2 %, for the logistic regression approach (LR-FM), random forest-FlamMap heat approach (RF-FM), and random forest-VIIRS approach (RF-VIIRS), respectively (Table 4). The RF-VIIRS approach had lower omission errors for both dead (11.2 %) and live (46.5 %) classes compared to the LR-FM approach (dead: 33.7–46.0 %, live: 40.9–55.2 %) and RF-FM approach (dead: 16.1–17.4 %, live: 70.0–70.8 %). Likewise, the RF-VIIRS approach had lower commission errors for both dead (20.4 %) and live (29.8 %) classes compared to the LR-FM approach (dead: 27.8–29.7 %, live: 59.7–60.5 %) and RF-FM approach (dead: 29.0–30.3 %, live: 52.2–54.0 %) (Table 4). The assessment of predictor variable importance for both random forest models shows that the fire intensity metrics (maximum FRP, FRE, modeled heat flux) were more important for live or dead classification than species or structural metrics (height, crown base height, Hegyi competition index) (Fig. 7). RF-FM models using 80th and 95th percentile fuel moisture and weather conditions had an identical order of predictor variable importance.

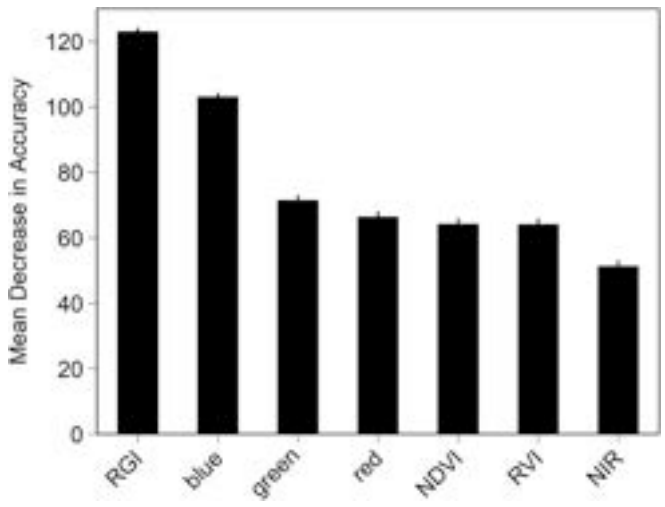

Fig. 6. Predictor variable importance reported as the mean (±95 % confidence interval) decrease in crown classification accuracy. RGI: Red-Green Index; blue: blue band; green: green band; red: red band; NDVI: Normalized Difference Vegetation Index; RVI: Ratio Vegetation Index; NIR: near infrared band. (For interpretation of the references to color in this figure legend, the reader is referred to the web version of this article.)

Table 4
Confusion matrix results showing live or dead classification accuracy for the logistic regression approach (LR-FM), random forest-FlamMap approach (RF-FM), and random forest-VIIRS approach (RF-VIIRS). Accuracy metrics for the LR-FM and RF-FM models report results for models using 80th and 95th percentile fuel moisture and weather conditions. Accuracy metrics for the random forest models report the mean (±95 % confidence interval), averaged across the 100 classification iterations.

Live or Dead classification	Accuracy metric	LR-FM (80th)	LR-FM (95th)	RF-FM (80th)	RF-FM (95th)	RF-VIIRS
Dead	Omission error (%)	46.0	33.7	17.4 (0.08)	16.1 (0.2)	11.2 (0.1)
	Commission error (%)	27.8	29.7	30.3 (0.05)	29.0 (0.1)	20.4 (0.1)
Live	Omission error (%)	40.9	55.2	70.8 (0.12)	70.0 (0.2)	46.5 (0.1)
	Commission error (%)	60.5	59.7	54.0 (0.11)	52.2 (0.2)	29.8 (0.2)
	Overall accuracy (%)	55.7	59.0	64.5 (0.05)	66.1 (0.1)	77.2 (0.1)

4.3. Uncertainty quantification and class attribution confidence analysis

The predicted and observed proportion of mortality by height size class across all fires is shown in Fig. 8. The RF-VIIRS model had the lowest RMSE and bias (6.3 % and 1.7 %, respectively), whereas the RF-FM and LR-FM model had higher RMSE and bias (RMSE: 10.2–38.4 %, bias: −29.6–3.7). All models overpredicted the proportion of mortality for smaller trees and underpredicted the proportion of mortality for larger trees, though error was much smaller for the random forest models (Fig. 8b,c) versus the logistic regression model (Fig. 8a). Predicted mortality RMSE and bias were lower for the random forest models for the fires that burned in 2023 (RMSE: 5.6–9.7 %, bias: 1.9–3.1 %) versus 2022 (RMSE: 8.3–13.3 %, bias: 6.6–8.1 %) (Fig. 9). Conversely, LR-FM predicted mortality RMSE and bias were higher for fires that burned in 2023 (RMSE: 39.9 %, bias: −31.2 %) versus 2022 (RMSE: 26.9 %, bias: -15.3 %).

Aggregated mortality error calculated as the difference in predicted minus observed total mortality (all size classes) for each 90 m grid cell within each fire, varied widely among the different models (Fig. 10). The RF-VIIRS model mortality error distribution was clustered closer to zero and had lower standard deviation (Fig. 10a; mean error ± SD: 7.9 ± 14.0 %) than the RF-FM model (Fig. 10b; mean error ± SD: 14.1 ± 25.4 %) and the LR-FM model (Fig. 10c; mean error ± SD: −22.8 ± 33.4 %). Overall, the majority of grid cells had a predicted total mortality that was underpredicted by the LR-FM approach and overpredicted by the RF approaches. Fig. 11 shows the aggregated mortality predictions and error, in terms of total observed mortality proportion per grid cell (Fig. 11a) and predicted mortality proportion per grid cell (Fig. 11b-d), across the southern extent of the 2023 Niarada fire. Notably, both the LR-FM and RF-FM approaches had higher error at the edges of the fire compared to the RF-VIIRS approach. Overall, the RF-VIIRS produced mortality patterns (Fig. 11f) that were qualitatively more similar to the observed mortality patterns (Fig. 11a) compared to the LR-FM (Fig. 11b) or RF-FM (Fig. 11d) results. Similar mortality prediction error patterns were observed for the other study fires.

Mortality prediction error decreased with increasing mean grid cell D2SC for the RF-FM model (Fig. 12a) and the RF-VIIRS model (Fig. 12b). The mortality prediction error variability also decreased with increasing D2SC, evidenced by the decreasing interquartile ranges with increasing D2SC (Fig. 12a,b).

5. Discussion

This study sought to predict the post-fire mortality of over 1.9 million trees in a mixed conifer forest using remotely sensed and modeled fire intensity and tree attributes from an ALS-derived individual tree inventory. Model predictions for individual tree mortality were validated using a reference dataset generated using high resolution NAIP imagery for each tree crown. The random forest classifiers outperformed the logistic regression approach with higher overall classification accuracy (RF-VIIRS: 77.2 %, RF-FM: 64.5–66.1 %, LR-FM: 55.7–59 %) and lower RMSE (RF-VIIRS: 6.3 %, RF-FM: 11.8 %, LR-FM: 41.3 %) and bias (RF-VIIRS: 1.7 %, RF-FM: 2.5 %, LR-FM: −35.2 %) when compared by tree size class. The predictor variable importance quantification showed that fire intensity metrics were the most important variables in the mortality classification. This study and others highlight the importance of fire intensity metrics for predicting post-fire individual tree mortality (Steady et al., 2019; Sparks et al., 2023b). Ultimately, this study demonstrated the utility of a remote sensing-based methodology for predicting tree mortality across large spatial extents that could potentially help managers proactively manage forests to reduce losses of merchantable timber volume and plan post-fire actions such as salvage logging and replanting operations. Following further validation in a wider diversity of fire-affected forest and woodland ecosystems, the RF approaches have the potential to be widely adopted to create a spatial product to predict fire-induced tree mortality across large spatial scales, providing end-users with a robust alternative to current fire severity geospatial products.

Predicting post-fire tree mortality using remote sensing data provides several key strengths over current approaches. First and foremost, predictions of mortality provide forest managers tools for proactive management instead of reactive management. While remote sensing data such as Landsat and small satellite data (e.g., PlanetScope) have enabled accurate mapping of post-fire stand scale mortality (Furniss et al., 2020) and crown scale mortality (Dixon et al., 2023) these data do not provide information that managers can use to take actions to reduce mortality prior to planned prescribed fires and unplanned wildfires. Clearly, the RF-FM approach would enable actions well in advance of unplanned fires, unlike the RF-VIIRS approach which relies on active fire data. However, the RF-VIIRS approach could provide useful information on where actions could be taken to reduce delayed mortality, which can occur many years after the fire (Youngblood et al., 2009), as well as inform post-fire remediation planning. Secondly, predicting individual tree mortality using ALS-derived inventories provides spatial context to the mortality estimation. Information on spatial patterns of tree

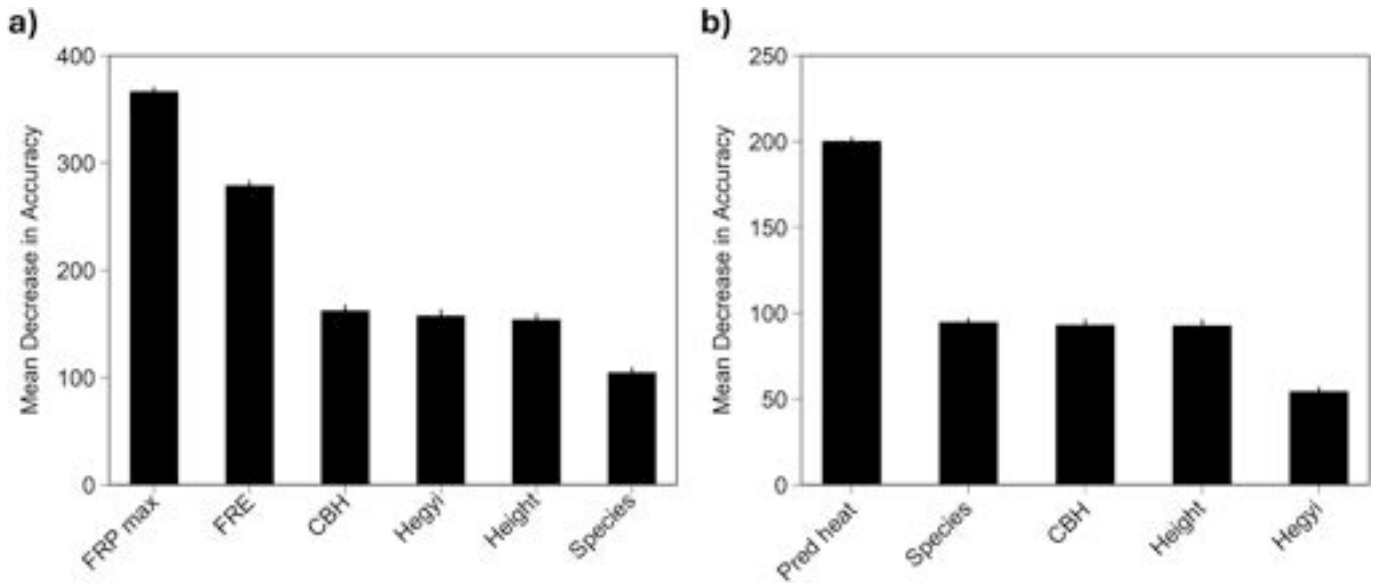

Fig. 7. Predictor variable importance reported as the mean (±95 % confidence interval) decrease in live or dead classification accuracy for the RF-VIIRS model (a) and the RF-FM model using 95th percentile fuel moisture and weather conditions (b). FRP max: maximum Fire Radiative Power; FRE: Fire Radiative Energy; CBH: crown base height, Hegyi: Hegyi competition index; Height: total tree height; Species: individual tree species; Pred heat: FlamMap predicted heat per unit area.

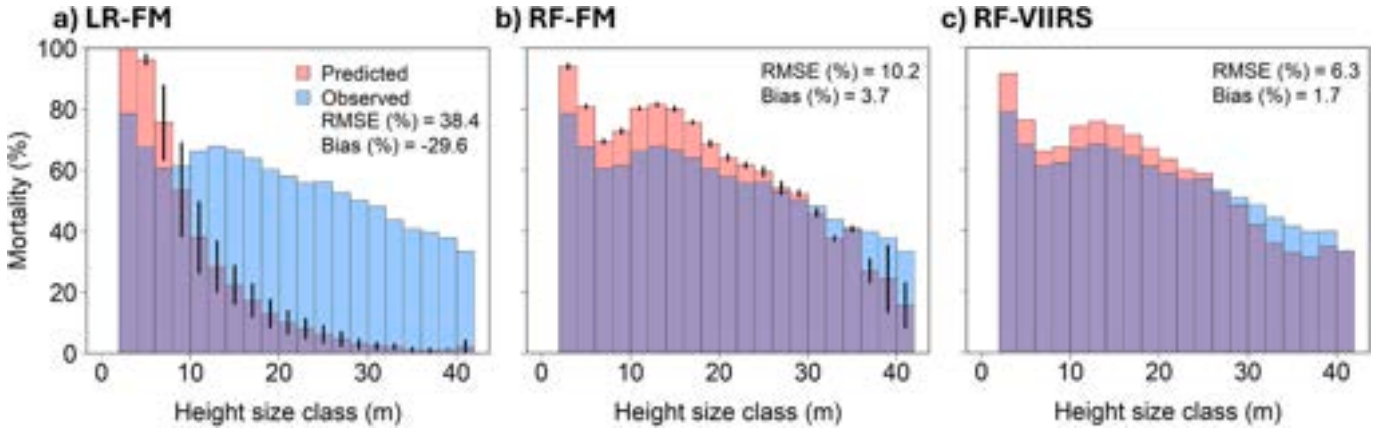

Fig. 8. Predicted and observed proportion of mortality by height size class across all fires. Panel (a) shows the LR-FM model predicted mortality versus observed mortality, (b) shows the RF-FM model predicted mortality versus observed mortality, and (c) shows the RF-VIIRS predicted mortality versus observed mortality. In (a) and (b) the error bars show the lower and upper predicted mortality bounds when using 80th and 95th percentile fuel moisture and weather conditions. In all panels, purple coloration indicates where the two distributions overlap. (For interpretation of the references to color in this figure legend, the reader is referred to the web version of this article.)

mortality is needed for silvicultural treatment planning to reduce expected mortality or plan for post-fire timber salvage and replanting operations (O'Brien et al., 2018; Keefe et al., 2022). For example, managers could use this information to identify where fires could cause the loss of significant timber volume resources, wildlife habitat or other ecosystem goods and services. While current approaches such as FVS-FFE provide estimates of stand level mortality, they do not provide information on how mortality varies over space (O'Brien et al., 2018). The distance to second class metric computed for the RF models also appears to provide key value added, spatially explicit information that managers and researchers can use to understand classification confidence. Class confidence information would be especially useful in areas with limited validation data that can be used to compute error estimates.

Remotely sensed fire intensity and tree attributes enhanced the accuracy of the mortality predictions. The RF-VIIRS model, which used VIIRS derived maximum FRP and FRE, was the most accurate model and these intensity metrics were identified as the two most important variables in the variable importance analysis. Likewise, ALS-derived height and distance-dependent competition were important for the RF-VIIRS and RF-FM classifiers. It is important to note that while some variables are ranked as more important than others, the output predictions rely on all predictor variables. However, the predictor variables ranked as more important coincided with expectations based on the fire induced tree mortality literature. For example, the relationship between fire intensity and tree mortality is well known (Ryan and Reinhardt, 1988; Smith et al., 2025). Other studies have also shown size-dependent relationships where smaller trees are killed at higher proportions than larger, more developmentally mature trees (Stephens and Finney, 2002; McDowell et al., 2018). Competition is also known to influence the post-fire mortality of conifers. For example, van Mantgem et al. (2016) observed significantly lower mortality in lower density stands, which they posited was due to reduced competition. The random forest models outperformed the logistic regression approach, which has also been observed using field-derived mortality datasets (Shearman et al., 2019). However, the random forest models still had relatively large omission errors for living trees, which may not be useful for some applications,

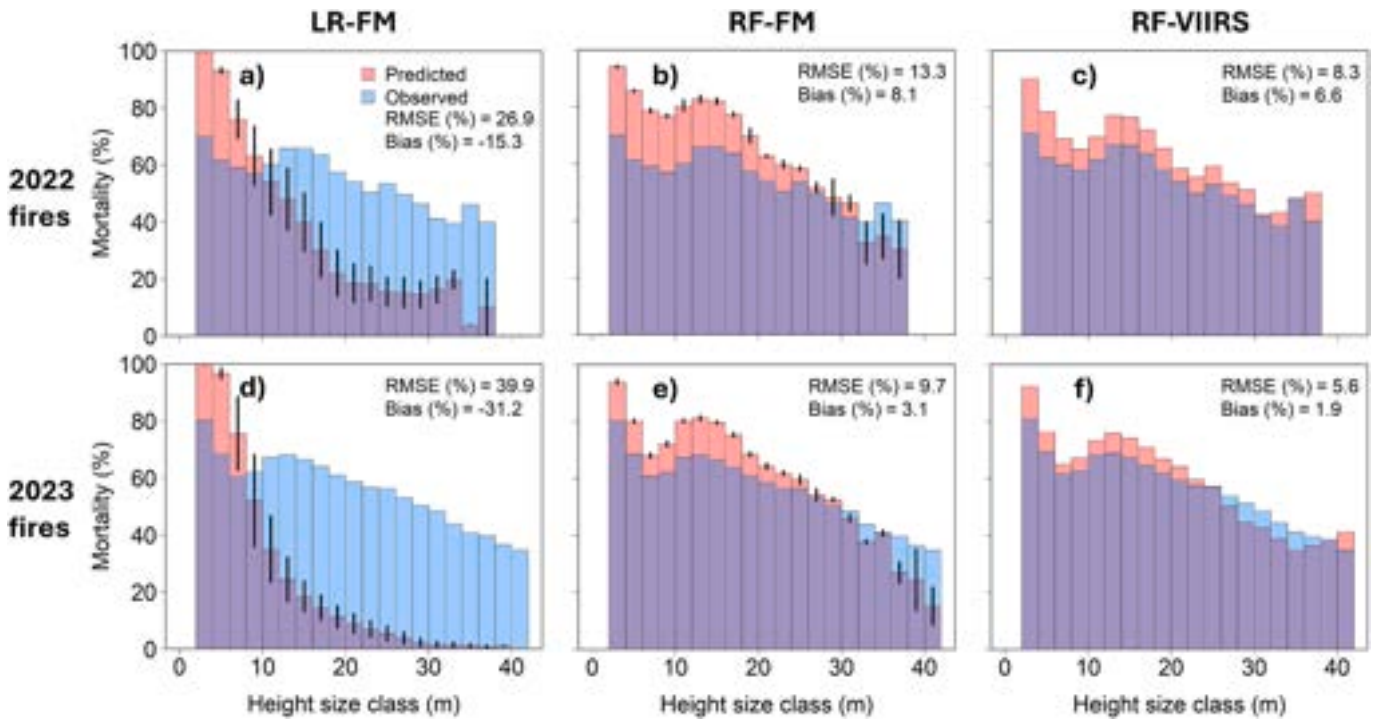

Fig. 9. Predicted and observed proportion of mortality by height size class across fires that burned in 2022 (top row) and fires that burned in 2023 (bottom row). Panels (a) and (d) show the LR-FM model predicted mortality versus observed mortality for 2022 and 2023, respectively. Panels (b) and (e) show the RF-FM model predicted mortality versus observed mortality. Panels (c) and (f) show the RF-VIIRS model predicted mortality versus observed mortality. For LR-FM and RF-FM panels, the error bars show the lower and upper predicted mortality bounds when using 80th and 95th percentile fuel moisture and weather conditions. In all panels, purple coloration indicates where the two distributions overlap. (For interpretation of the references to color in this figure legend, the reader is referred to the web version of this article.)

such as predicting survival of legacy trees (Cansler et al., 2020). While machine learning models such as random forest are more difficult to interpret than other modeling approaches (Cutler et al., 2007), forest managers may be more interested in accurate prediction over interpretability (Shearman et al., 2019). Given observations showing that stressed trees have a greater mortality probability than non-stressed trees (van Mantgem et al., 2013; van Mantgem et al., 2016; Partelli-Feltrin et al., 2020; Sparks et al., 2024b) further work could explore using remotely sensed datasets that can quantify drought stress, such as ECOSTRESS evaporative stress index (Fisher et al., 2011, 2020), to increase the accuracy of post-fire mortality prediction.

While this study developed a promising remote sensing-based methodology for predicting individual fire-induced tree mortality, several limitations should be explored in future research. Firstly, this study relied on high pulse density ALS data (mean 20 ppm) to identify and segment the individual tree crowns. Availability of similar datasets may preclude this methodology from being implemented in other areas. While there is freely available lower pulse density ALS data (~8 ppm), such as the United States Geological Survey (USGS) 3D Elevation Program (US Geological Survey, 2024), some of these collections may be inaccurate for segmenting crowns due to forest disturbances between the date of ALS collection, and high-resolution imagery date. However, the growing use of uncrewed aerial systems-based ALS data may also help fill gaps where ALS data is not available. Furthermore, Digital Aerial Photogrammetric (DAP) point clouds derived from stereo imagery may serve as another potential dataset that could be used to fill in gaps between ALS datasets. For example, the segmentation of NAIP-derived canopy height models could potentially supplement current ALS acquisitions, given its ability to quantify stand height (Strunk et al., 2019; Ritz et al., 2022), and acquisition frequency of 2–3 years for entire conterminous United States. Another limitation that should be considered is the error associated with individual tree detection and segmentation derived from ALS data. The individual tree detection methodology used in this study has higher detection rates of dominant and codominant trees and lower detection rates of intermediate and suppressed trees (Sparks et al., 2022; Sparks et al., 2022). These detection rates will likely produce less accurate results in cases where the mortality rate of smaller trees occluded by the overstory are needed (i.e., quantifying mortality of smaller trees that constitute crown ladder fuels).

Other limitations of the presented methodology include its reliance on modeled attributes that have not been validated widely. Due to various constraints, validation of several of the input datasets, including surface fuel model selection and crown base height was not conducted in this study. The accuracy of the FVS-FFE surface fuel model selection is not well understood. However, several studies have compared custom fuel models derived from field data to the FVS-FFE selected generalized fuel models and found that although the custom fuel models more accurately represented actual fuel loads, the resulting modeled fire behavior was not significantly different (Noonan-Wright et al., 2014; Barker et al., 2019). The uncertainty associated with FVS-FFE modeled tree crown ratio is also not well understood. Tinkham et al. (2017) found FVS-FFE modeled crown ratio was underestimated by approximately 5 % to 20 % depending on site index for conifers in the central Rocky Mountains, USA. This observed crown ratio underestimation resulted in an overestimation of CBH. To help reduce the CBH overestimation error in the current study we adjusted the crown bulk density threshold from 0.011 kg m^{-3} to 0.005 kg m^{-3}.

Wildfires are stochastic events and are highly variable in space and time, and managers do not know the exact weather and fuel moisture conditions under which future wildfires will burn. To address this uncertainty, managers could use this methodology to model a range of fire weather and fuel conditions to more accurately capture this variability. In this study, we modeled fire behavior for 80–95th percentile scenarios

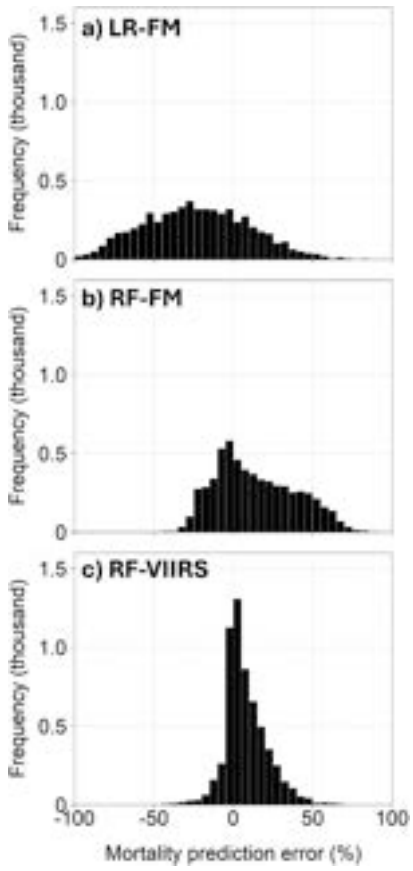

Fig. 10. The distribution of mortality prediction error, calculated as the difference in predicted minus observed total mortality (all size classes) for each 90 m grid cell across all study fires. Panels (a–c) show the error distribution for the LR-FM, RF-FM, and RF-VIIRS models, respectively. In (a) and (b) the mortality prediction error is shown for the average of the models using 80th and 95th percentile fuel moisture and weather conditions.

to capture a broad range of fire behavior. However, depending on the application of the prediction, different modeled ranges may be more useful. For example, predicting mortality of fire-susceptible species may require fire behavior modeling using more conservative fuel moisture and weather conditions. Another consideration of using methodology that incorporates active fire observations is that due to the high spatial and temporal heterogeneity of fire behavior, a lower active fire observation frequency can result in a poorer characterization of the fire behavior (Giglio, 2007; Freeborn et al., 2014; Hudak et al., 2015). This study incorporated VIIRS observations from only the Suomi-NPP and NOAA-20 satellites as VIIRS data from NOAA-21 was not available for this study. Combined observations from all three satellites could potentially improve the fire characterization of future work and the resulting tree mortality prediction accuracy. In addition to temporal considerations, the relatively coarse resolution of VIIRS data relative to the scale of individual trees likely increases mortality prediction error as the coarse scale data overpredicts intensity for some trees and underpredicts intensity for others.

Like other studies, our findings show that the timing of mortality classification is an important consideration for predicting mortality. In general, delayed mortality is much more difficult to predict than immediate mortality as additional stressors (e.g., drought, competition, insects) increase the probability of tree mortality after the fire (Kane et al., 2017; Hood et al., 2018). In part due to these additional factors, morphologically based predictions of tree mortality have been shown to degrade in accuracy over time (Shearman et al., 2023). As NAIP imagery is collected every 2–3 years, this data could be used to examine the relationship between individual tree attributes, fire intensity and delayed mortality. The random forest classification results from this study also show that classifying mortality for older fires (>1 year before NAIP imagery acquisition) can be a source of error (Fig. 9). Specifically, understory regeneration in older fires caused some of the segmented tree crowns to appear healthy, when they were visibly defoliated in the post-fire high resolution NAIP imagery. Future studies could use post-fire ALS data to screen out trees with consumed crowns by assessing the reduction of crown volume within each segmented tree crown from pre-fire to post-fire.

6. Conclusions

This study demonstrated that integrating remotely sensed and modeled fire intensity data with ALS derived data has considerable potential to develop new spatially explicit fire-induced tree mortality products. Through the use of an ALS-derived individual tree inventory of over 1.9 million trees this study highlights the valuable structural information that high-resolution ALS data (>20 ppm) can provide to fire management and forest management planning efforts. Integration of modeled fire intensity suggests that this methodology is adaptable to simulate multiple fire modeling scenarios, which could be used to more fully understand the variability in fire behavior and tree mortality across space. Future research could also assess whether the inclusion of other information, such as remotely sensed measures of chlorophyll fluorescence and water stress that have been shown to be indicators of drought-based tree mortality (Fisher et al., 2011, 2020; Guadagno et al., 2017), aids in increasing the mortality prediction accuracy. Equally, inclusion of ancillary datasets such as down-scaled vapor pressure deficit, gridded surface winds, and soil moisture should be explored. The framework presented in this study has considerable potential to advance fire severity research beyond the over-reliance on NBR and similar spectral indices that lack a mechanistic connection to the fire-affected ecosystems toward the creation of the next-generation of robust and validated remote sensing products to predict and assess fire impacts on trees. Such products need to be robustly validated across a wide range of fire-affected ecosystems and should leverage planned fire behavior and remote sensing field campaigns, such as that proposed by the National Aeronautics and Space Administration FireSense program (Falkowski et al., 2024).

The development of accurate regional fire-induced tree mortality products could also enable significant improvements in the creation of tertiary products related to the assessment of above and below ground carbon emissions and stocks following fires (Stenzel et al., 2019), the modeling of biogeochemical cycles (Hanan et al., 2022), predicting the risk of future wildfire ignitions associated with dead trees falling on power lines (Ahmed et al., 2013), evaluating impacts on growth and yield (Sparks et al., 2023b), and modeling potential fire impacts associated with erosion and slope stability (Abdollahi et al., 2023). The creation of these tertiary application products would be achieved through coupling the spatially explicit fire-induced tree mortality data with other datasets related to topography, soil properties, and hydrology that could also be acquired through remote sensing.

CRediT authorship contribution statement

Aaron M. Sparks: Writing – review & editing, Writing – original draft, Visualization, Validation, Formal analysis, Conceptualization. **Ryan Armstrong:** Writing – review & editing, Formal analysis, Data curation. **Alistair M.S. Smith:** Writing – review & editing, Conceptualization. **Steve Scharosch:** Writing – review & editing, Data curation. **Mark V. Corrao:** Writing – review & editing, Data curation, Conceptualization. **Thomas Montzka:** Writing – review & editing, Data curation.

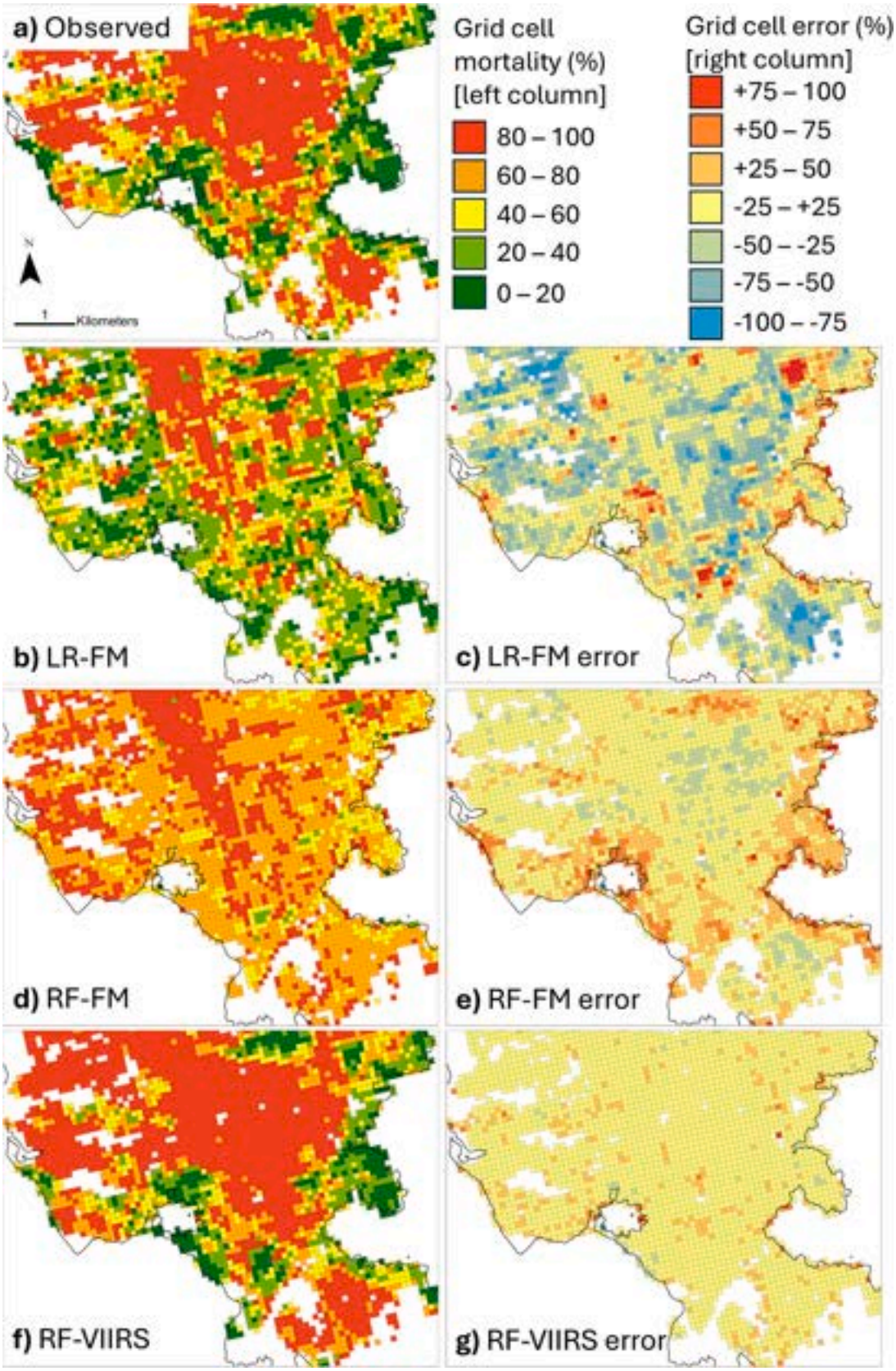

Fig. 11. Total mortality (left panes) and predicted mortality error (right panes) aggregated to each 90 m grid cell across the southern extent of the 2023 Niarada fire. Panel (a) shows the observed mortality and panels (b,d,f) show the predicted mortality for the LR-FM, RF-FM, and RF-VIIRS models, respectively. Panels (c,e,g) show the predicted mortality error for the LR-FM, RF-FM, and RF-VIIRS models, respectively. Only grid cells within the fire perimeter that contain trees are shown.

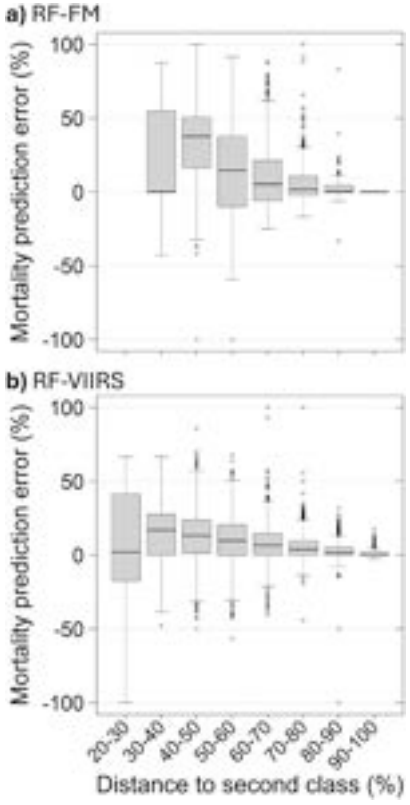

Fig. 12. Mortality prediction error for each 90 m grid cell across all study fires binned by distance to second class (D2SC). Values of D2SC closer to 0 indicate lower class attribution confidence while values closer to 100 indicate higher class attribution confidence. Panel (a) shows the mortality prediction error by D2SC bin for the average of the RF-FM models using 80th and 95th percentile fuel moisture and weather conditions. Panel (b) shows the mortality prediction error by D2SC bin for the RF-VIIRS model.

Declaration of competing interest

The authors declare the following financial interests/personal relationships which may be considered as potential competing interests.

Acknowledgements

The authors thank Northwest Management Incorporated (NMI, Moscow, Idaho) for providing the ALS datasets. Partial funding for Sparks was provided by the National Institute of Food and Agriculture, USDA, McIntire Stennis project under IDAZ-CNR-0618 and the National Science Foundation award 2418257. Smith was funded by the National Aeronautics and Space Administration under the FireSense project 80NSSC24K1305.

Data availability

Data will be made available on request.

References

Abatzoglou, J.T., Battisti, D.S., Williams, A.P., Hansen, W.D., Harvey, B.J., Kolden, C.A., 2021. Projected increases in western US forest fire despite growing fuel constraints. Commun. Earth Environ. 2, 1–8.
Abdollahi, M., Vahedifard, F., Tracy, F.T., 2023. Post-wildfire stability of unsaturated hillslopes against rainfall-triggered landslides. Earth's Future 11 (3), e2022EF003213.
Ager, A.A., Finney, M.A., Kerns, B.K., Maffei, H., 2007. Modeling wildfire risk to northern spotted owl (Strix occidentalis caurina) habitat in Central Oregon, USA. For. Ecol. Manag. 246, 45–56.
Ager, A.A., Vaillant, N.M., Finney, M.A., 2010. A comparison of landscape fuel treatment strategies to mitigate wildland fire risk in the urban interface and preserve old forest structure. For. Ecol. Manag. 259, 1556–1570.
Ahmed, J., Malik, A.S., Xia, L., Ashikin, N., 2013. Vegetation encroachment monitoring for transmission lines right-of-ways: a survey. Electr. Power Syst. Res. 95, 339–352.
Alcasena, F.J., Salis, M., Nauslar, N.J., Aguinaga, A.E., Vega-García, C., 2016. Quantifying economic losses from wildfires in black pine afforestations of northern Spain. Forest Pol. Econ. 73, 153–167.
Andela, N., Morton, D.C., Giglio, L., Chen, Y., van der Werf, G.R., Kasibhatla, P.S., DeFries, R.S., Collatz, G.J., Hantson, S., Kloster, S., Bachelet, D., 2017. A human-driven decline in global burned area. Science 356 (6345), 1356–1362.
Andrews, P.L., 1986. BEHAVE: Fire Behavior Prediction and Fuel Modeling System — BURN Subsystem Part 1. USDA For. Serv (Gen Tech. Rep. INT-194.).
ASPRS, 2011. ASPRS LAS Format Standard 1.4. Available online: https://www.asprs.org/wp-content/uploads/2019/07/LAS_1_4_r15.pdf (accessed on 9 December 2024).
Barker, J.S., Fried, J.S., Gray, A.N., 2019. Evaluating model predictions of fire induced tree mortality using wildfire-affected forest inventory measurements. Forests 10, 958.
Boschetti, L., Roy, D.P., 2009. Strategies for the Fusion of Satellite Fire Radiative Power with Burned Area Data for Fire Radiative Energy Derivation. J. Geophys. Res.-Atmos. 114.
Bowman, D.M., Williamson, G.J., Abatzoglou, J.T., Kolden, C.A., Cochrane, M.A., Smith, A.M.S., 2017. Human exposure and sensitivity to globally extreme wildfire events. Nature Ecol. Evol. 1, 0058.
Breiman, L., 2001. Random forests. Mach. Learn. 45, 5–32.
Brown, J.K., 1978. Weight and density of crowns of Rocky Mountain conifers. Res. Pap. INT-197. Ogden, UT: U.S. Department of Agriculture, Forest Service, intermountain Forest and range Experiment Station.
Cansler, C.A., Hood, S.M., van Mantgem, P.J., Varner, J.M., 2020. A large database supports the use of simple models of post-fire tree mortality for thick-barked conifers, with less support for other species. Fire Ecol. 16, 1–37.
Contreras, M.A., Affleck, D., Chung, W., 2011. Evaluating tree competition indices as predictors of basal area increment in western Montana forests. For. Ecol. Manag. 262, 1939–1949.
Coops, N.C., Johnson, M., Wulder, M.A., White, J.C., 2006. Assessment of QuickBird high spatial resolution imagery to detect red attack damage due to mountain pine beetle infestation. Remote Sens. Environ. 103, 67–80.
Corrao, M.V., Sparks, A.M., Smith, A.M.S., 2022. A conventional cruise and felled-tree validation of individual tree diameter, height and volume derived from airborne laser scanning data of a loblolly pine (P. Taeda) stand in eastern Texas. Remote Sens 14, 2567.
Cutler, D.R., Edwards Jr., T.C., Beard, K.H., Cutler, A., Hess, K.T., Gibson, J., Lawler, J.J., 2007. Random forests for classification in ecology. Ecology 88, 2783–2792.
Dickman, L.T., Jonko, A.K., Linn, R.R., Altintas, I., Atchley, A.L., Bär, A., Collins, A.D., Dupuy, J.L., Gallagher, M.R., Hiers, J.K., Hoffman, C.M., 2023. Integrating plant physiology into simulation of fire behavior and effects. New Phytol. 238, 952–970.
Dixon, D.J., Zhu, Y., Brown, C.F., Jin, Y., 2023. Satellite detection of canopy-scale tree mortality and survival from California wildfires with spatiotemporal deep learning. Remote Sens. Environ. 298, 113842.
Ellis, T.M., Bowman, D.M., Jain, P., Flannigan, M.D., Williamson, G.J., 2022. Global increase in wildfire risk due to climate-driven declines in fuel moisture. Glob. Chang. Biol. 28, 1544–1559.
Falkowski, M.J., Smith, A.M.S., Gessler, P.E., Hudak, A.T., Vierling, L.A., Evans, J.S., 2008. The influence of conifer forest canopy cover on the accuracy of two individual tree measurement algorithms using lidar data. Can. J. Remote. Sens. 34, S338–S350.
Falkowski, M.J., Shuman, J., Boland, J., Kauffman, T., Lefer, B., Martin, M.M., 2024. The NASA FireSense Project: Responding to Stakeholder Needs Across the Fire Life Cycle. In: IGARSS 2024–2024 IEEE International Geoscience and Remote Sensing Symposium, Athens, Greece, pp. 2356–2359. https://doi.org/10.1109/IGARSS53475.2024.10642820.
Finney, M.A., 2006. An Overview of FlamMap Fire Modeling Capabilities. InFuels Management—How to Measure Success: conference proceedings (Vol. 28, p. 30). USDA Forest Service, Rocky Mountain Research Station, Fort Collins, CO.
FireFamily+, 2024. Fire family plus. Available at https://www.firelab.org/project/firefamilyplus (last access: 11 November 2024), 2024.
Fisher, J.B., Whittaker, R.J., Malhi, Y., 2011. ET come home: potential evapotranspiration in geographical ecology. Glob. Ecol. Biogeogr. 20, 1–18.
Fisher, J.B., Lee, B., Purdy, A.J., Halverson, G.H., Dohlen, M.B., Cawse-Nicholson, K., Wang, A., Anderson, R.G., Aragon, B., Arain, M.A., Baldocchi, D.D., 2020. ECOSTRESS: NASA'S next generation mission to measure evapotranspiration from the international space station. Water Resour. Res. 56, e2019WR026058.
Flanary, S.J., Keane, R.E., 2020. Ponderosa pine mortality in the bob Marshall wilderness after successive fires over 14 years. Research note. RMRS-RN-85. Fort Collins, CO: U.S. Department of Agriculture, Forest Service. Rocky Mountain Research Station.
Freeborn, P.H., Wooster, M.J., Roy, D.P., Cochrane, M.A., 2014. Quantification of MODIS fire radiative power (FRP) measurement uncertainty for use in satellite-based active fire characterization and biomass burning estimation. Geophys. Res. Lett. 41, 1988–1994.
Furniss, T.J., Kane, V.R., Larson, A.J., Lutz, J.A., 2020. Detecting tree mortality with Landsat-derived spectral indices: improving ecological accuracy by examining uncertainty. Remote Sens. Environ. 237, 111497.
Gesch, D., Oimoen, M., Greenlee, S., Nelson, C., Steuck, M., Tyler, D., 2002. The national elevation dataset. Photogramm. Eng. Remote. Sens. 68, 5–32.
Giglio, L., 2007. Characterization of the tropical diurnal fire cycle using VIRS and MODIS observations. Remote Sens. Environ. 108, 407–421.

Giglio, L., Schroeder, W., Justice, C.O., 2016. The collection 6 MODIS active fire detection algorithm and fire products. Remote Sens. Environ. 178, 31–41.
Guadagno, C.R., Ewers, B.E., Speckman, H.N., Aston, T.L., Huhn, B.J., DeVore, S.B., Ladwig, J.T., Strawn, R.N., Weinig, C., 2017. Dead or alive? Using membrane failure and chlorophyll a fluorescence to predict plant mortality from drought. Plant Physiol. 175 (1), 223–234.
Hanan, E.J., Kennedy, M.C., Ren, J., Johnson, M.C., Smith, A.M.S., 2022. Missing climate feedbacks in fire models: limitations and uncertainties in fuel loadings and the role of decomposition in fine fuel accumulation. J. Advances Modeling Earth Sys. 14 (3), e2021MS002818.
Hegyi, F., 1974. A simulation model for managing jackpine stands. In: Fries, J. (Ed.), Proceedings of IUFRO meeting S4.01.04 on growth models for tree and stand simulation. Royal College of forestry, Stockholm.
Hemming-Schroeder, N.M., Gutierrez, A.A., Allison, S.D., Randerson, J.T., 2023. Estimating individual tree mortality in the Sierra Nevada using lidar and multispectral reflectance data. J. Geophys. Res.-Biogeosciences 128 (5) e2022JG007234.
Hermosilla, T., Bastyr, A., Coops, N.C., White, J.C., Wulder, M.A., 2022. Mapping the presence and distribution of tree species in Canada's forested ecosystems. Remote Sens. Environ. 282, 113276.
Hood, S.M., 2010. Mitigating old tree mortality in long-unburned, fire-dependent forests: a synthesis. In: Gen. Tech. Rep. RMRS-GTR-238. Fort Collins, CO: US Department of Agriculture. Forest Service, Rocky Mountain Research Station.
Hood, S.M., Varner, J.M., Van Mantgem, P., Cansler, C.A., 2018. Fire and tree death: understanding and improving modeling of fire-induced tree mortality. Environ. Res. Lett. 13, 113004.
Hudak, A.T., Dickinson, M.B., Bright, B.C., Kremens, R.L., Loudermilk, E.L., O'Brien, J.J., Hornsby, B.S., Ottmar, R.D., 2015. Measurements relating fire radiative energy density and surface fuel consumption–RxCADRE 2011 and 2012. Int. J. Wildland Fire 25, 25–37.
Kane, J.M., Varner, J.M., Metz, M.R., van Mantgem, P.J., 2017. Characterizing interactions between fire and other disturbances and their impacts on tree mortality in western US forests. For. Ecol. Manag. 405, 188–199.
Keefe, R.F., Zimbelman, E.G., Picchi, G., 2022. Use of individual tree and product level data to improve operational forestry. Current Forest. Rep. 8, 148–165.
Kleinman, J.S., Goode, J.D., Fries, A.C., Hart, J.L., 2019. Ecological consequences of compound disturbances in forest ecosystems: a systematic review. Ecosphere 10, e02962.
LANDFIRE: LANDFIRE Existing Vegetation Type layer, 2023. U.S. Department of Interior (update 2023). Geological Survey available at: https://www.landfire.gov/viewer/ (last access: 11 November 2024).
Liaw, A., Wiener, M., 2002. Classification and regression by randomforest. R News 2, 18–22. https://CRAN.R-project.org/doc/Rnews/.
Linn, R.R., Goodrick, S.L., Brambilla, S., Brown, M.J., Middleton, R.S., O'Brien, J.J., Hiers, J.K., 2020. QUIC-fire: a fast-running simulation tool for prescribed fire planning. Environ. Model Softw. 125, 104616.
Lorimer, C.G., 1983. Tests of age-independent competition indices for individual trees in natural hardwood stands. For. Ecol. Manag. 6, 343–360.
Lutes, Duncan, 2020. FOFEM 6.7 first order fire effects model user guide, fire and aviation management. Fort Collins: USDA Rocky Mountain Research Station fire modelling institute. Updated September 20, 2023. https://www.firelab.org/document/fofem-files.
Lyons, M.B., Keith, D.A., Phinn, S.R., Mason, T.J., Elith, J., 2018. A comparison of resampling methods for remote sensing classification and accuracy assessment. Remote Sens. Environ. 208, 145–153.
Maxwell, A.E., Warner, T.A., Vanderbilt, B.C., Ramezan, C.A., 2017. Land cover classification and feature extraction from National Agriculture Imagery Program (NAIP) Orthoimagery: a review. Photogramm. Eng. Remote. Sens. 83, 737–747.
McDowell, N.G., Michaletz, S.T., Bennett, K.E., Solander, K.C., Xu, C., Maxwell, R.M., Middleton, R.S., 2018. Predicting chronic climate-driven disturbances and their mitigation. Trends Ecol. Evol. 33, 15–27.
Mell, W., Jenkins, M.A., Gould, J., Cheney, P., 2007. A physics-based approach to modelling grassland fires. Int. J. Wildland Fire 16 (1), 1–22.
Mitchell, S.W., Remmel, T.K., Csillag, F., Wulder, M.A., 2008. Distance to second cluster as a measure of classification confidence. Remote Sens. Environ. 112 (5), 2615–2626.
Noonan-Wright, E.K., Vaillant, N.M., Reiner, A.L., 2014. The effectiveness and limitations of fuel modeling using the fire and fuels extension to the Forest vegetation simulator. For. Sci. 60, 231–240.
O'Brien, J.J., Hiers, J.K., Varner, J.M., Hoffman, C.M., Dickinson, M.B., Michaletz, S.T., Loudermilk, E.L., Butler, B.W., 2018. Advances in mechanistic approaches to quantifying biophysical fire effects. Current Forest. Rep. 4, 161–177.
Partelli-Feltrin, R., Johnson, D.M., Sparks, A.M., Adams, H.D., Kolden, C.A., Nelson, A.S., Smith, A.M.S., 2020. Drought increases vulnerability of Pinus ponderosa saplings to fire-induced mortality. Fire 3 (4), 56.
Pearson, R.L., Miller, L.D., 1972. Remote mapping of standard crop biomass for estimation of the productivity of the shortgrass prairie, Pawnee National Grasslands, Colorado. In: Proceedings of the 8th international symposium on remote sensing of the environment, II, pp. 1355–1379.
Peterson, D.L., Ryan, K.C., 1986. Modeling postfire conifer mortality for long-range planning. Environ. Manag. 10 (6), 797–808.
R Core Team, 2024. R: A Language and Environment for Statistical Computing. R Foundation for Statistical Computing, Vienna, Austria.
Rebain, Stephanie A., 2022. The Fire and Fuels Extension to the Forest Vegetation Simulator: Updated Model Documentation; Internal Report. USDA Forest Service, Forest Management Service Center, Fort Collins, CO. https://www.fs.usda.gov/fmsc/ftp/fvs/docs/gtr/FFEguide.pdf.
Ritz, A.L., Thomas, V.A., Wynne, R.H., Green, P.C., Schroeder, T.A., Albaugh, T.J., Burkhart, H.E., Carter, D.R., Cook, R.L., Campoe, O.C., Rubilar, R.A., 2022. Assessing the utility of NAIP digital aerial photogrammetric point clouds for estimating canopy height of managed loblolly pine plantations in the southeastern United States. Int. J. Appl. Earth Obs. Geoinf. 113, 103012.
Rothermel, R.C., 1972. A mathematical model for predicting fire spread in wildland fuels. In: USDA Forest Service research paper INT-115.
Rouse, J.W., Haas, R.H., Schell, J.A., Deering, D.W., Harlan, J.C., 1974. Monitoring the Vernal Advancements and Retrogradation of Natural Vegetation. NASA/GSFC, Final Report: Greenbelt, MD, USA, p. 137.
Ryan, K.C., Reinhardt, E.D., 1988. Predicting postfire mortality of seven western conifers. Canadian J. Forest Res. 18, 1291–1297.
Schroeder, W., Ellicott, E., Ichoku, C., Ellison, L., Dickinson, M.B., Ottmar, R.D., Clements, C., Hall, D., Ambrosia, V., Kremens, R., 2014a. Integrated active fire retrievals and biomass burning emissions using complementary near-coincident ground, airborne and spaceborne sensor data. Remote Sens. Environ. 140, 719–730.
Schroeder, W., L. Giglio, 2016. Visible Infrared Imaging Radiometer Suite (VIIRS) 375 m Active Fire Detection and Characterization Algorithm Theoretical Basis Document 1.0. Available online (accessed October 31,2024): https://viirsland.gsfc.nasa.gov/PDF/VIIRS_activefire_375m_ATBD.pdf.
Schroeder, W., Oliva, P., Giglio, L., Csiszar, I.A., 2014b. The new VIIRS 375 m active fire detection data product: algorithm description and initial assessment. Remote Sens. Environ. 143, 85–96.
Scott, J.H., Burgan, R.E., 2005. Standard Fire Behavior Fuel Models: A Comprehensive Set for Use with Rothermel's Surface Fire Spread Model. US Department of Agriculture, Forest Service, Rocky Mountain Research Station.
Shearman, T.M., Varner, J.M., Hood, S.M., Cansler, C.A., Hiers, J.K., 2019. Modelling post-fire tree mortality: can random forest improve discrimination of imbalanced data? Ecol. Model. 414, 108855.
Shearman, T.M., Varner, J.M., Hood, S.M., van Mantgem, P.J., Cansler, C.A., Wright, M., 2023. Predictive accuracy of post-fire conifer death declines over time in models based on crown and bole injury. Ecological App. 33, e2760.
Shive, K.L., Wuenschel, A., Hardlund, L.J., Morris, S., Meyer, M.D., Hood, S.M., 2022. Ancient trees and modern wildfires: declining resilience to wildfire in the highly fire-adapted giant sequoia. For. Ecol. Manag. 511, 120110.
Smith, A.M.S., Talhelm, A.F., Johnson, D.M., Sparks, A.M., Kolden, C.A., Yedinak, K.M., Apostol, K.G., Tinkham, W.T., Abatzoglou, J.T., Lutz, J.A., Davis, A.S., 2017. Effects of fire radiative energy density dose on Pinus contorta and Larix occidentalis seedling physiology and mortality. Int. J. Wildland Fire 26, 82–94.
Smith, A.M.S., Partelli-Feltrin, R., Sparks, A.M., Moberly, J.G., Adams, H.D., Schwilk, D. W., Tinkham, W.T., Kok, J.R., Wilson, D.R., Alex Thompson, R., Hudak, A.T., Hoffman, C.M., Lutz, J.A., Blanco, A.S., Cochrane, M.A., Kremens, R.L., Dahlen, J., Harley, G.L., Rainsford, S.W., Huang, L., Hardman, D.D., Boschetti, L., Johnson, D. M., 2025. Methods to assess fire-induced tree mortality: review of fire behavior proxy and real fire experiments. Int. J. Wildland Fire 34.
Sofan, P., Bruce, D., Schroeder, W., Jones, E., Marsden, J., 2020. Assessment of VIIRS 375 m active fire using tropical peatland combustion algorithm applied to Landsat-8 over Indonesia's peatlands. Int. J. Digital Earth 13, 1695–1716.
Sparks, A.M., Smith, A.M.S., 2022. Accuracy of a lidar-based individual tree detection and attribute measurement algorithm developed to inform forest products supply chain and resource management. Forests 13, 3.
Sparks, A.M., Kolden, C.A., Smith, A.M.S., Boschetti, L., Johnson, D.M., Cochrane, M.A., 2018. Fire intensity impacts on post-fire temperate coniferous forest net primary productivity. Biogeosciences 15, 1173–1183.
Sparks, A.M., Corrao, M.V., Smith, A.M.S., 2022. Cross-comparison of individual tree detection methods using low and high pulse density airborne laser scanning data. Remote Sens 14, 3480.
Sparks, A.M., Blanco, A.S., Wilson, D.R., Schwilk, D.W., Johnson, D.M., Adams, H.D., Bowman, D.M., Hardman, D.D., Smith, A.M.S., 2023a. Fire intensity impacts on physiological performance and mortality in Pinus monticola and Pseudotsuga menziesii saplings: a dose–response analysis. Tree Physiol. 43, 1365–1382.
Sparks, A.M., Smith, A.M.S., Hudak, A.T., Corrao, M.V., Kremens, R.L., Keefe, R.F., 2023b. Integrating active fire behavior observations and multitemporal airborne laser scanning data to quantify fire impacts on tree growth: a pilot study in mature Pinus ponderosa stands. Forest Ecology Manage. 545, 121246.
Sparks, A.M., Corrao, M.V., Keefe, R.F., Armstrong, R., Smith, A.M.S., 2024a. An Accuracy Assessment of Field and Airborne Laser Scanning–Derived Individual Tree Inventories using Felled Tree Measurements and Log Scaling Data in a Mixed Conifer Forest. For. Sci. 70, 228–241.
Sparks, A.M., Blanco, A.S., Lad, L.E., Smith, A.M.S., Adams, H.D., Tinkham, W.T., 2024b. Prefire drought intensity drives postfire recovery and mortality in Pinus monticola and Pseudotsuga menziesii saplings. For. Sci. 70, 189–201.
Sparks, A.M., Smith, A.M., Talhelm, A.F., Kolden, C.A., Yedinak, K.M., Johnson, D.M., 2017. Impacts of fire radiative flux on mature Pinus ponderosa growth and vulnerability to secondary mortality agents. International Journal of Wildland Fire 26 (1), 95–106.
Steady, W.D., Partelli Feltrin, R., Johnson, D.M., Sparks, A.M., Kolden, C.A., Talhelm, A. F., Lutz, J.A., Boschetti, L., Hudak, A.T., Nelson, A.S., Smith, A.M.S., 2019. The survival of Pinus ponderosa saplings subjected to increasing levels of fire behavior and impacts on post-fire growth. Fire 2, 23.
Stenzel, J.E., Bartowitz, K.J., Hartman, M.D., Lutz, J.A., Smith, A.M.S., Kolden, C.A., Law, B.E., Swanson, M.E., Larson, A.J., Parton, W.J., 2019. Fixing a snag in estimating carbon emissions from wildfires. Glob. Chang. Biol. 25, 3985–3994.

Stephens, S.L., Finney, M.A., 2002. Prescribed fire mortality of Sierra Nevada mixed conifer tree species: effects of crown damage and forest floor combustion. For. Ecol. Manag. 162, 261–271.
Stovall, A.E., Shugart, H., Yang, X., 2019. Tree height explains mortality risk during an intense drought. Nature communications 10 (1), 4385.
Strunk, J., Packalen, P., Gould, P., Gatziolis, D., Maki, C., Andersen, H.E., McGaughey, R. J., 2019. Large area forest yield estimation with pushbroom digital aerial photogrammetry. Forests 10, 397.
Tinkham, W.T., Hoffman, C.M., Ex, S., Smith, A.M.S., 2017. Sensitivity of crown fire modeling to inventory parameter dubbing in FVS. In: Proceedings of the 2017 Forest Vegetation Simulator (FVS) e-Conference. U.S. Department of Agriculture, Forest Service, Southern Research, Station: Asheville, NC, USA, pp. 114–123. General Technical Report, SRS-eGTR-224.
US Geological Survey, 2024. USGS National map 3DEP downloadable data collection. US Geological Survey. https://www.usgs.gov/3d-elevation-program.
van Lierop, P., Lindquist, E., Sathyapala, S., Franceschini, G., 2015. Global forest area disturbance from fire, insect pests, diseases and severe weather events. For. Ecol. Manag. 352, 78–88.
van Mantgem, P.J., Nesmith, J.C., Keifer, M., Knapp, E.E., Flint, A., Flint, L., 2013. Climatic stress increases forest fire severity across the western United States. Ecol. Lett. 16, 1151–1156.
van Mantgem, P.J., Caprio, A.C., Stephenson, N.L., Das, A.J., 2016. Does prescribed fire promote resistance to drought in low elevation forests of the Sierra Nevada, California, USA? Fire Ecol. 12, 13–25.
van Wagner, C.V., 1973. Height of crown scorch in forest fires. Canadian J. Forest Res. 3, 373–378.
Vauhkonen, J., Ene, L., Gupta, S., Heinzel, J., Holmgren, J., Pitkänen, J., Solberg, S., Wang, Y., Weinacker, H., Hauglin, K.M., Lien, V., 2012. Comparative testing of single-tree detection algorithms under different types of forest. Forestry 85, 27–40.
Voelker, S.L., Merschel, A.G., Meinzer, F.C., Ulrich, D.E., Spies, T.A., Still, C.J., 2019. Fire deficits have increased drought sensitivity in dry conifer forests: fire frequency and tree-ring carbon isotope evidence from Central Oregon. Glob. Chang. Biol. 25, 1247–1262.
Wolfe, R.E., Lin, G., Nishihama, M., Tewari, K.P., Tilton, J.C., Isaacman, A.R., 2013. Suomi NPP VIIRS prelaunch and on-orbit geometric calibration and characterization. Journal of Geophysical Research: Atmospheres 118 (20), 11–508.
Woolley, T., Shaw, D.C., Ganio, L.M., Fitzgerald, S., 2011. A review of logistic regression models used to predict post-fire tree mortality of western north American conifers. Int. J. Wildland Fire 21, 1–35.
Wooster, M.J., Zhukov, B., Oertel, D., 2003. Fire radiative energy for quantitative study of biomass burning: derivation from the BIRD experimental satellite and comparison to MODIS fire products. Remote Sens. Environ. 86, 83–107.
Wooster, M.J., Roberts, G.J., Giglio, L., Roy, D.P., Freeborn, P., Boschetti, L., Justice, C. O., Ichoku, C.M., Schroeder, W., Davies, D.K., Smith, A.M.S., Setzer, A., Csiszar, I., Strydom, T., Frost, P., Zhang, T., Xu, W., de Jong, M., Johnston, J.M., Ellison, L., Vadrevu, K.P., Sparks, A.M., Nguyen, H., McCarty, J.L., Tanpipat, V., Schmidt, C., San-Miguel-Ayanz, J., 2021. Satellite Remote Sensing of Active Fires: History and Current Status, Applications and Future Requirements. Remote Sens. Environ. 267.
Youngblood, A., Grace, J.B., McIver, J.D., 2009. Delayed conifer mortality after fuel reduction treatments: interactive effects of fuel, fire intensity, and bark beetles. Ecol. Appl. 19, 321–337.
Zhang, T., Wooster, M.J., Xu, W., 2017. Approaches for synergistically exploiting VIIRS I- and M-band data in regional active fire detection and FRP assessment: a demonstration with respect to agricultural residue burning in eastern China. Remote Sens. Environ. 198, 407–424.